



Study on Landslide Stability and Refined Risk Assessment of Taijiapo, Xinchang Village, Zhongping Town, Qianxi County, Guizhou Province

Guangya Luo

Guizhou Province Nonferrous Metal and Nuclear Industry Geological Survey Bureau No. 5 Corps, Anshun 560000, Guizhou, China

Abstract: This study, based on detailed geological disaster investigation and quantitative risk assessment techniques, takes the Taijiapo landslide in Xinchang Village, Zhongping Town, Qianxi County as the research object. Through engineering geological mapping, drilling, geophysical prospecting, and numerical simulation, the formation mechanism and risk characteristics of landslides in the red-bed area are revealed. The results show that the landslide is an extra-large, medium-layer translational rock–soil mixed landslide, with a volume of approximately 3.6 million m³ and a main sliding direction of 5°–10°; the sliding zone is the contact surface between silty clay and bedrock, with low shear strength (saturated state $c = 12$ kPa, $\varphi = 8^\circ$); under heavy rainfall conditions, the stability coefficient drops to 1.03–1.08, indicating a state of critical instability. Dynamic simulation based on the MassFlow model predicts a maximum sliding distance of 292 m, threatening 600 m of road. The study establishes a quantitative risk assessment system of “geological mechanism–stability–vulnerability,” providing a theoretical basis for the prevention and control of red-bed landslides.

Keywords: red-bed landslide; MassFlow simulation; risk zoning; northwest Qianxi

1. Introduction

1.1 Research Background

Zhongping Town in Qianxi County is the region with the most developed geological disasters in the county. Among them, the Taijiapo landslide in Xinchang Village, which occurred in July 2020, is a large red-bed landslide of typical research value, reflecting the basic characteristics and disaster patterns of geological hazards in the town. Since its formation, the landslide has been undergoing continuous creeping deformation, directly threatening 80 households and 281 people. As of July 12 of the same year, it had caused 24 households' houses to collapse or suffer severe damage, 13 households' houses to deform, with direct economic losses of approximately 8.5 million yuan and potential economic losses reaching 24 million yuan. The disaster and risk levels were both classified as large-scale. On July 10, 2020, monitoring personnel discovered cracks and deformation from the mountain pass to Fujiawan Road and promptly reported it. The local authorities completed the evacuation of residents by 18:00 on the same day, avoiding casualties.

At present, academia has conducted extensive research on the formation mechanism, disaster-causing factors, monitoring, and early warning of shallow soil landslides [1,2,3], and has made progress in landslide distance prediction and numerical simulation parameters [4,5]. However, most studies focus on regional-scale hazard assessment [6,7], while quantitative evaluation of individual landslides remains insufficient. Due to advantages such as low cost and convenience, numerical simulation has become an important method for studying the landslide movement process [8,9,10]. For example, Lu [11] used PFC3D to simulate the rolling path and deposition range of unstable mountain masses in Taiwan, while Ouyang [12], Zhou Qi [13], and Song Deguang [14] applied the MassFlow model to invert or analyze the movement processes of Baige Landslide, Heifangtai Chenjia Landslide, and Haiziping Landslide in Luding, Sichuan, respectively. With the improvement of computing power, numerical simulation plays an increasingly prominent role in inverting and predicting landslide movement characteristics, sliding distance, and hazard range, promoting the in-depth development of related research [15,16,17,18].

Therefore, based on the specialized geological investigation and monitoring data of the Taijiapo landslide in Zhongping Town, Qianxi County, this study systematically summarizes the developmental characteristics and deformation evolution of red-bed landslides. It integrates UAV aerial survey (1 km²) and Lidar data (6.7 km²) to construct a three-dimensional geological model with centimeter-level accuracy. Using the MassFlow software, the entire landslide movement process was parametrically simulated, with a focus on analyzing the dynamic behavior under heavy rainfall conditions (daily rainfall >100 mm).

1.2 Research Content and Methods

Integrating geological investigation reports and quantitative risk assessment technical documents, a multi-dimensional analysis framework was adopted:

(1) Geological Investigation: Engineering surveying (1:1000 topographic mapping), drilling (139.78 m), mountain engineering (25 m³ exploratory trenches), and geotechnical testing (12 groups of soil samples).

(2) Risk Assessment: MassFlow dynamic simulation, vulnerability quantification model, and risk zoning.

2. Geological Environment and Landslide Characteristics

2.1 Geological Environmental Conditions

The Taijiapo landslide is located in the Fujiawan Formation of Xinchang Village, Zhongping Town, Qianxi County, Guizhou Province, with geographic coordinates of E106°16'30", N27°09'45" (center point). The annual average temperature ranges from 14.5°C to 22.8°C. The area receives abundant precipitation, with an annual average rainfall of 947 mm. Heavy rainfall mainly occurs from May to August (accounting for 74% of the annual precipitation), and high-intensity rainfall during the rainy season significantly intensifies landslide deformation activity. The landslide is situated on the east bank of a tributary of the Wujiang River, characterized by a medium-incised, stepped gentle slope geomorphology. The landslide area is controlled by the Gemuxiang syncline and regional faults (see Figure 1). The Gemuxiang syncline is arched northeastward (axial direction 30°), and the regional fault is a west-dipping, medium-angle thrust fault (dip 55°–65°). The combined effect of these two geological structures forms the structural basis for slope instability.

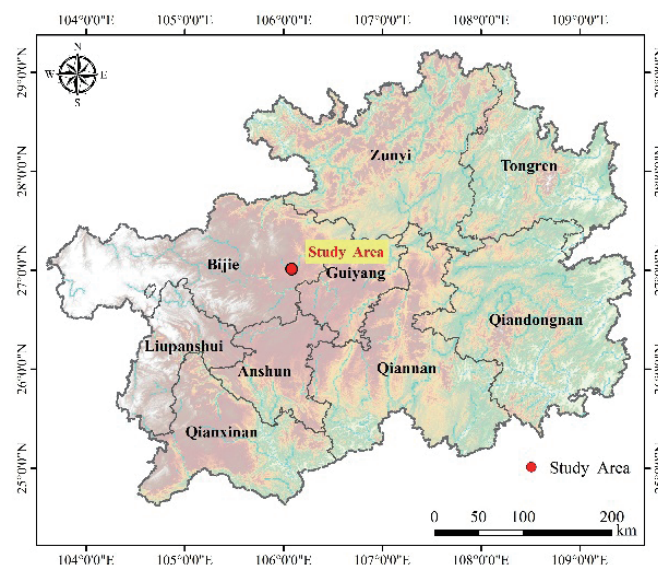


Figure 1. Geographic Location of the Study Area

2.2 Basic Characteristics of the Landslide

2.2.1 Landslide Boundaries

(1) Rear Boundary: Located near the contact between the rear of the slope body and the road, presenting a southwestward convex arc, with ground elevations of 1310–1315 m. The rear of the landslide exposes claystone of the Ziliujing Formation, with a bedding attitude of $345^\circ \angle 15^\circ$, forming a bedding-parallel slope. The bedrock slope exhibits relatively good stability.

(2) Front Boundary: The gullies on both sides converge from the middle-rear section to the front, and the convergence point marks the front boundary.

(3) Lateral Boundaries: Based on field investigation, gullies develop on both sides of the landslide. Considering the extent of tensile cracks, the lateral boundaries of the landslide are determined by the gullies.

2.2.2 Morphological Characteristics and Scale of the Landslide

The main sliding direction of the landslide is 5°–10°, with a tongue-shaped planform. The longitudinal slope length is 1,200 m, the transverse width ranges from 100 to 300 m, the landslide area is 240,000 m², and the average thickness of the sliding mass is 10–25 m, with a volume of approximately 3.6×10^6 m³, classifying it as a large-scale landslide.

2.2.3 Characteristics of the Sliding Mass

Based on geological profile mapping, drilling, and trenching data, the landslide material mainly consists of purplish-red to flesh-red clay–silty clay, with minor gravel particles and yellowish claystone fragments. The surface shows occasional calcareous nodules, plant roots, and minor limestone clasts. Vertically, the sliding mass is thicker in the middle and front and thinner at the rear, generally 10–25 m thick, with a maximum thickness of 28 m. Horizontally, the thickness is relatively uniform, ranging from 15 to 22 m. Some boreholes near the sliding mass reveal multiple sliding planes, suggesting that the landslide may have experienced multiple sliding events (Figure 2).

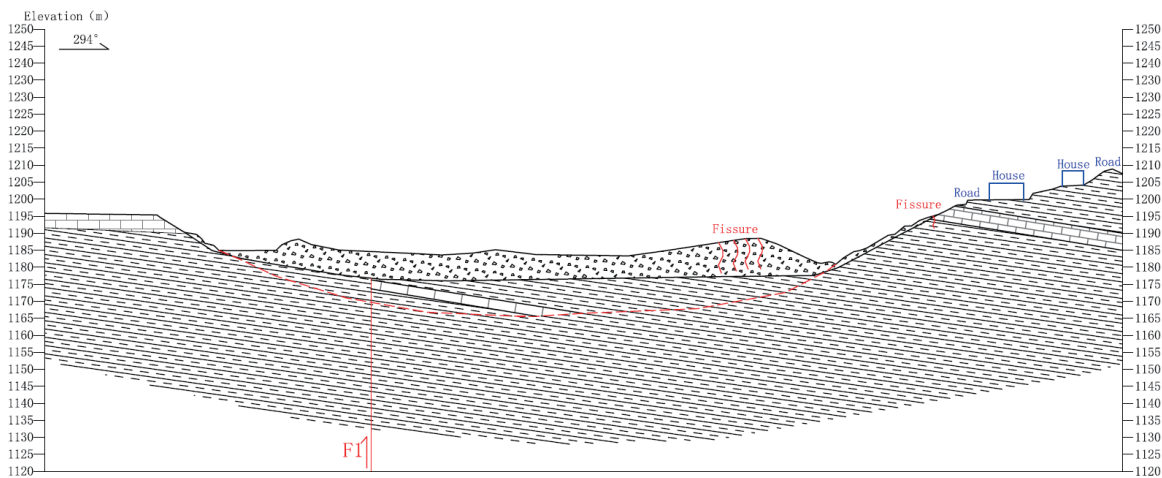


Figure 2. Engineering Geological Profile

2.3 Deformation Characteristics of the Landslide

Since its formation, the landslide experienced severe deformation and failure from July 8 to July 10, 2020. After a temporary base was laid with plastic sheets, the deformation gradually stabilized. Currently, the landslide mass remains in a creeping state, and under conditions such as heavy rainfall, it is highly likely that deformation and failure will be exacerbated, potentially triggering further sliding. Additionally, due to tensile cracking and compressive deformation observed in the rear rock mass, and bulging deformation caused by soil compression in the middle and front sections, it is comprehensively determined that the landslide is an extra-large, medium-layer translational rock–soil mixed landslide.

Overall, the current landslide in Xinchang Village, Zhongping Town, can be divided into three zones: the initiation zone, the collision zone, and the translational zone (see Figure 3), each exhibiting different deformation characteristics and degrees of damage.



Figure 3. Zoning Map of Landslide Deformation Intensity

The initiation zone is located at the rear of the landslide mass, where tensile cracks are well developed, with an overall strike of 70°–90° and a width generally ranging from 0.3 to 1 m. In some areas, multiple cracks have combined to form crack zones, with a maximum width of up to 5 m and a gradually widening trend. In the central part of this zone, a tensile subsidence trench has developed, with staggered heights of 2–3 m and an extension length of 30–40 m. In front of the tensile subsidence trench, multiple levels of staggered steep scarps have formed, with height differences of 1–3 m. Additionally, houses in this area show varying degrees of cracking at the front, rear, and interiors; some have tilted or even collapsed. Field investigation also identified a spring in this zone, with groundwater discharge, although the flow rate is relatively small.

The collision zone is located in the middle of the landslide, where damage to houses and roads is most severe. Tensile cracks are less developed, some houses have completely collapsed, and roads show uplift and displacement. Influenced by the initiation zone, this area has experienced a high level of destructive energy overall.

The translational zone is located at the front of the landslide. Under the push from the middle and rear sections, the front-edge displacement is mainly along the main sliding direction. One house was displaced approximately 40 m but did not suffer overall destruction. In other areas, bounded by gullies on both sides, tongue-shaped bulging occurs, with multiple farmlands showing radial cracks. The overall thickness of the cover layer is relatively large, consistent with the observations from borehole ZK6.

3. Establishment of the MassFlow Numerical Model

3.1 Introduction to the MassFlow Model

MassFlow software is based on depth-integrated continuum mechanics theory and uses an improved MacCormack-TVD finite difference method. It is an efficient computational simulation tool for mountain disasters, capable of considering complex terrain and topography, with second-order accuracy and adaptive solution domain features. Numerical simulation based on the dynamic process can reveal the spatiotemporal evolution of mountain disasters, providing theoretical and technical support for quantitative risk assessment of mountain hazards, infrastructure and urban planning, and the formulation of disaster reduction, prevention, and relief strategies [19,20].

3.2 Analysis of Motion Parameters

To ensure computational accuracy and precision, selecting a model with fewer parameters can reduce the workload of disaster surveying and improve computational efficiency. In this simulation, a basal friction model based on the Coulomb model was established. This model requires three parameters: cohesion, basal friction coefficient, and pore water pressure coefficient. Generally, during high-speed sliding, the cohesion between soil particles can be approximately neglected. The pore water pressure ranges from 0 (dry gravel state) to 1 (fully saturated debris flow state), with its generation and dissipation affecting the expansion of soil particles and water diffusion. The basal friction coefficient is related to key landslide motion parameters, including maximum horizontal travel distance (L_{max}), horizontal travel distance at the slope toe (L_1), and landslide movement distance (L_2). L_{max} and L_1 are the primary evaluation indicators for landslide disaster prevention and mitigation.

In this simulation, the sliding zone material of the Taijiapo landslide in Xinchang Village mainly consists of silty clay with gravel, with gravel particle sizes of 1–3 cm, sub-rounded in shape, and lithology of metamorphic sandstone and schist. These data provide important reference for the average friction coefficient. Under the most unfavorable conditions, the basal average friction coefficient for the Taijiapo landslide was set at 0.4.

Based on obtained imagery, field survey data, and combined results from drilling and geophysical prospecting, a numerical simulation model of the landslide was established, using a 5 m × 5 m square grid for calculations (Figure 4).

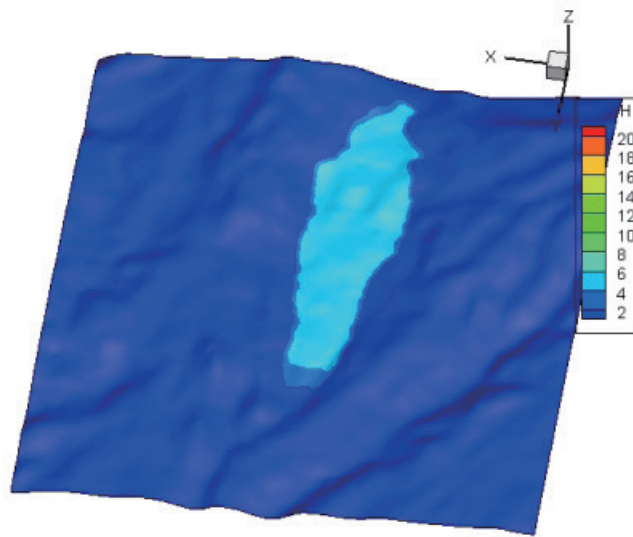


Figure 4. 3D MassFlow Model of the Landslide

4. Stability Analysis and Risk Assessment

4.1 Quantitative Stability Calculation

The sliding surface, identified as the weak plane through combined field and laboratory analysis, is polyline-shaped. Therefore, the stability calculation adopts the polyline sliding surface formula, and the residual downslope force is calculated using the transfer coefficient method.

The stability calculation formulas follow the polyline approach, and the stability coefficient k is calculated using formulas (1)–(4) as follows:

$$F_s = \frac{\sum_{i=1}^n (R_i \prod_{j=i}^{n-1} \psi_j) + R_n}{\sum_{i=1}^n (T_i \prod_{j=i}^{n-1} \psi_j) + T_n} \quad (1)$$

$$\psi_j = \cos(\theta_i - \theta_{i+1}) - \sin(\theta_i - \theta_{i+1}) \tan \phi_{i+1} \quad (2)$$

$$\prod_{j=i}^{n-1} \psi_j = \psi_i \bullet \psi_{i+1} \bullet \psi_{i+2} \cdots \bullet \psi_{n-1} \quad (3)$$

$$R_i = N_i \tan \phi_i + C_i L_i \quad (4)$$

F_s ——Stability Coefficient;

Q_i ——Resistance Acting on the i th Segment of the Sliding Mass;

R_i ——Sliding Resistance Acting on the i th Segment;

N_i ——Normal Force on the Sliding Surface of the i th Segment;

ϕ_i ——Internal Friction Angle ($^\circ$) of the i th Segment of Soil;

C_i ——Cohesion (kPa) of the i th Segment of Soil;

L_i ——Length of the Sliding Surface of the i th Segment (m);

T_i ——Sliding Force Acting on the i th Segment of the Sliding Surface (kN/m); when the sliding force acts opposite to the sliding direction, T_i should be taken as a negative value

ψ_j ——Transfer Coefficient for Residual Downslope Force from the i th Segment to the $i+1$ th Segment ($j = i$).

ψ_j ——Transfer Coefficient of Residual Downslope Force from the i th Segment to the $i+1$ th Segment ($j = i$).

The calculation results are shown in Table 1:

Table 1. Calculated Stability Results of the Landslide

Calculation Profile	Failure Mode	Natural Condition (k)	Saturated Condition (k)	Remarks
3-3'	Type I	1.47	1.19	
	Type II	2.10	1.71	
	Type III	1.35	1.10	

4.2 Landslide Stability Evaluation

The overall stability of the landslide was calculated and analyzed, and the results are generally consistent with the actual conditions of the landslide. The evaluation is based on the standards in the Specifications for Survey of Landslide Prevention and Control Engineering: stability coefficient $K < 1.0$ indicates an unstable state; $1.0 \leq K < 1.05$ indicates a marginally unstable state; $1.05 \leq K < 1.15$ indicates a basically stable state; $K \geq 1.15$ indicates a stable state. Through the calculation and analysis of landslide profile 3-3', the following conclusions can be drawn:

(1) Under the three failure modes, except for the saturated condition in the third failure mode where the stability coefficient is below 1.10, indicating a basically stable state, the stability coefficients in all other conditions for the three failure modes are greater than 1.15, indicating a stable state.

(2) The Taijiapo landslide in Xinchang Village, Zhongping Town, identified in this investigation, is a typical translational landslide. Since the dip angle of the strata in such landslides is much smaller than the internal friction angle, according to the traditional limit equilibrium theory, a landslide of such large scale is unlikely to occur on a near-horizontal bedrock slope without special causes. Because other influencing factors were not considered in this theoretical analysis, the overall stability coefficient is relatively high.

4.3 Landslide Hazard Assessment Based on MassFlow

4.3.1 Analysis of Simulation Results

Under the most unfavorable conditions, the Taijiapo landslide in Xinchang Village exhibits the following engineering impact range: through numerical calculations, the simulated deposition of the landslide body at $T = 10$ s, 30 s, 50 s, and 80 s under the most unfavorable conditions is shown in Figure 5.

The simulation results indicate that the overall slope is relatively steep, especially in the middle-rear and front sections, with considerable thickness of the sliding mass. At $T = 10$ s, material from the steep rear section rapidly slides downward, while a small amount at the front edge begins to shear out toward the riverbed, with a cumulative sliding distance of approximately 50 m. At $T = 30$ s, material from the rear section has largely accumulated in the middle of the landslide, with an accumulation thickness of about 9.14 m; the speed gradually decreases, and the cumulative sliding distance at the front edge reaches approximately 80 m. The area of maximum sliding velocity has largely shifted to the front edge. At $T = 50$ s, the rear and middle sections have basically reached stable accumulation, with a thickness of about 10.82 m, while the front edge still maintains high speed, depositing in the riverbed, with a cumulative sliding distance of approximately 154 m. At $T = 80$ s, the landslide as a whole has nearly ceased movement. Due to the large volume, thick deposits are present both on the slope and in the riverbed, with a deposition thickness of about 19.11 m and a cumulative sliding distance of approximately 292 m.

4.3.2 Hazard Zoning

Based on the analysis of landslide motion characteristics from MassFlow numerical simulation, and verified through field investigation, the landslide hazard is classified into four levels — very high, medium, and low — using the impact force of the sliding mass as the criterion. The resulting hazard zoning map of the Taijiapo landslide in Xinchang Village is shown in Figure 6.

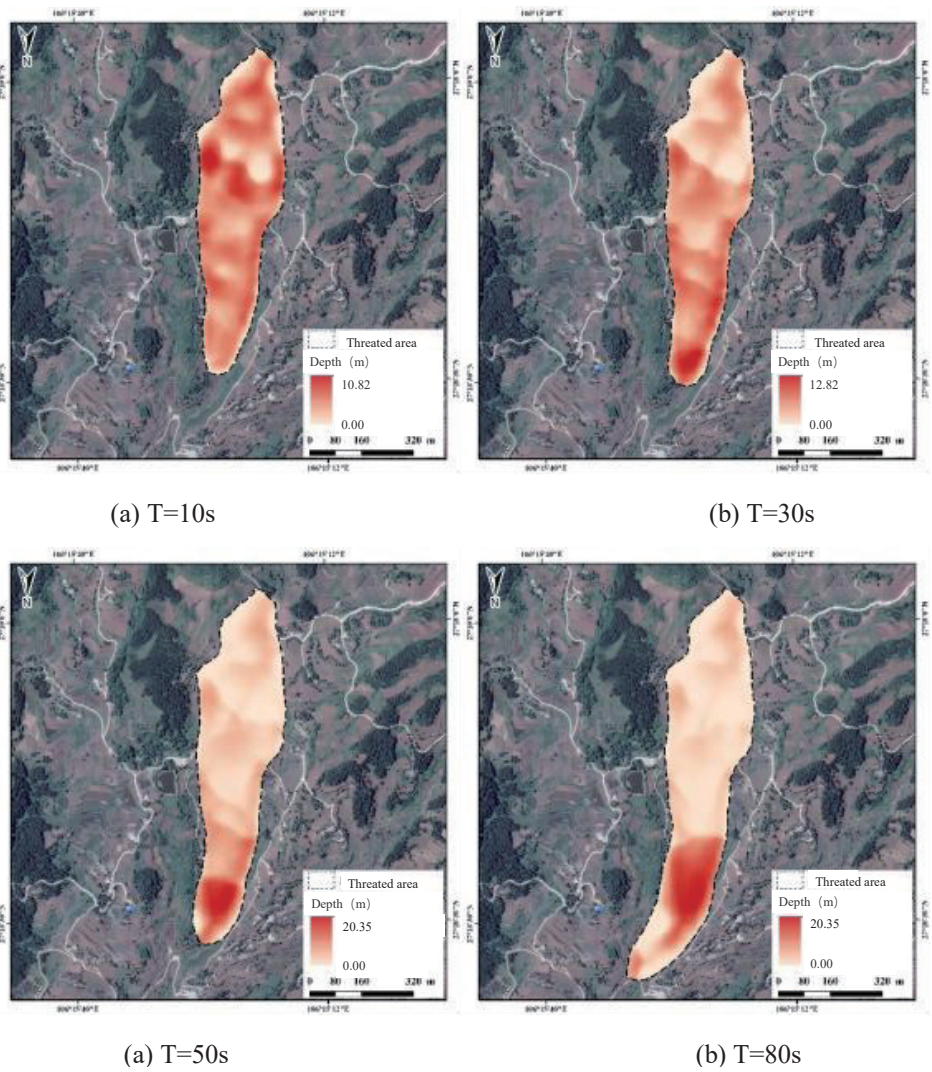


Figure 5. MassFlow Simulation of the Taijiapo Landslide in Xinchang Village at Different Times

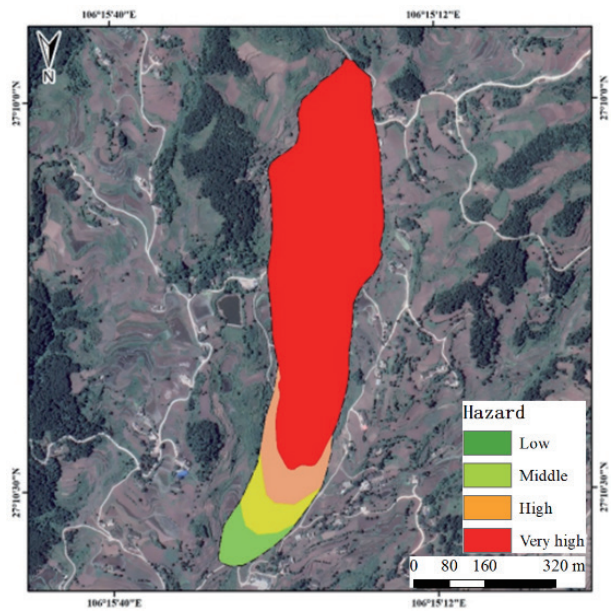


Figure 6. Hazard Zoning Map of the Taijiapo Landslide in Xinchang Village

4.3.3 Vulnerability Assessment

The threats posed by geological disasters can be mainly divided into two categories: human casualties and economic losses. Based on this, vulnerability assessment indicators can be selected from four major categories:

(1) Material Vulnerability: Refers primarily to infrastructure and buildings, which are tangible assets. The greater the value of fixed assets such as buildings and transportation facilities within the affected area, the larger the total material loss in the event of a natural disaster, and thus the higher the vulnerability.

(2) Economic Vulnerability: Refers to intangible assets. Since the study area is primarily rural with a coal-based, single-industry economy, household annual income was chosen as the indicator to evaluate economic vulnerability.

(3) Environmental Vulnerability: In this study, environmental vulnerability refers to the vulnerability of natural resources, with land resources considered the main carrier of environmental vulnerability.

(4) Social Vulnerability: Social vulnerability considers all the population within the affected area, including the social structure of these potentially affected people.

The vulnerability assessment of the Taijiapo landslide in Xinchang Village is as follows:

Based on the distribution of exposed elements within the landslide area, an attribute database of exposed elements for the Taijiapo landslide was established in Arcgis. Within the threat range of the landslide, there are no houses, population, or other exposed elements at risk—only a single road is present, with a total length of approximately 600 m, classified as a township or lower-level road. The vulnerability assessment results of the Taijiapo landslide in Xinchang Village are shown in Figure 7.

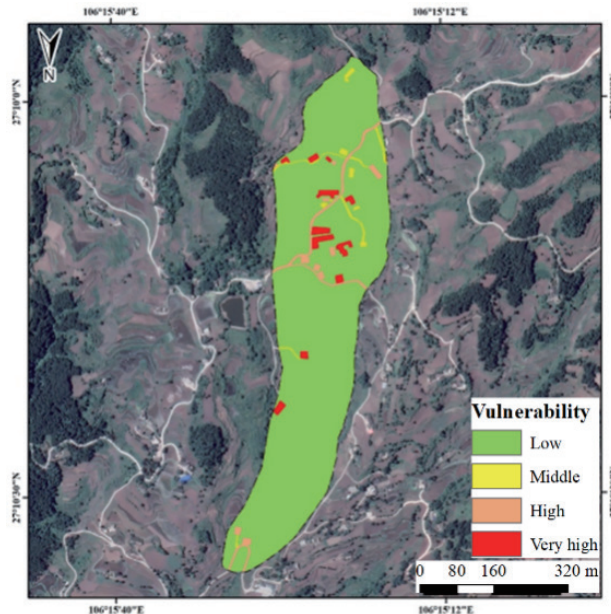


Figure 7. Vulnerability Zoning Map of the Taijiapo Landslide in Xinchang Village

4.3.4 Risk Assessment

Based on the results of individual geological disaster risk assessments and considering the actual conditions of the study area, risk zoning was conducted within the hazard range of each geological disaster point. The zones are classified into very high-risk, high-risk, medium-risk, and low-risk areas: Very high-risk areas indicate regions with concentrated population and property distribution, where various land types are highly susceptible to severe losses, posing serious threats to residents' lives. Infrastructure, ecological environment, and socio-economic activities are severely affected. High-risk areas indicate regions where exposed elements are highly likely to suffer disaster, causing significant losses and threatening residents' lives. Medium-risk areas indicate regions where exposed elements may suffer partial loss, affecting residents' daily life and causing moderate impacts on infrastructure, ecological environment, and socio-economic activities. Low-risk areas indicate regions with minimal residential activity and building distribution, where infrastructure, ecological environment, and socio-economic activities are little affected (Figure 8).

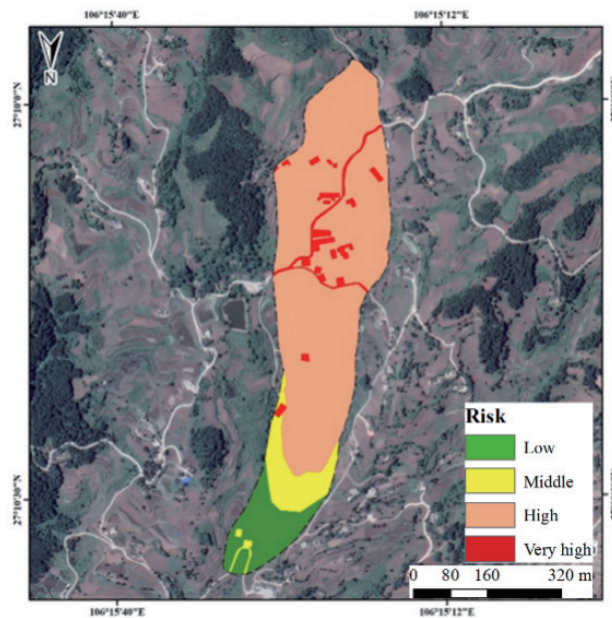


Figure 8. Risk Zoning Map of the Taijiapo Landslide in Xinchang Village

5. Conclusions

By analyzing the landslide structure and deformation characteristics of the Taijiapo landslide in Xinchang Village, Zhongping Town, Qianxi County, and through engineering geological mapping, drilling, geophysical prospecting, and numerical simulation, the formation mechanism and risk characteristics of landslides in the red-bed region were revealed. The main conclusions based on MassFlow dynamic simulation are as follows:

- (1) The landslide is a super-large, mid-layer translational rock-soil mixed landslide, with a volume of approximately $3.6 \times 10^6 \text{ m}^3$ and a main sliding direction of $5^\circ\text{--}10^\circ$;
- (2) The sliding zone is at the silty clay–bedrock interface, with low shear strength (saturated state: $c = 12 \text{ kPa}$, $\phi = 8^\circ$). Under heavy rainfall conditions, the stability coefficient drops to 1.03–1.08, indicating a critically unstable state;
- (3) MassFlow dynamic simulation predicts a maximum sliding distance of 292 m, threatening a road stretch of 600 m.

References

- [1] ZHANG Qun, XU Qiang, NING Na. A study of the stability influence factors and coupling for inclined-shallow soil landslides under the condition of rainfall[J]. *Hydrogeology & Engineering Geology*, 2014, 41(05): 90-94+117. (in Chinese)
- [2] WEI X, WEN F. Disaster law of shallow landslide in Qin-ba Mountain region[J]. *Journal of Catastrophology*, 2014.
- [3] QI Xing, XU Qiang, ZHENG Guang, et al. Dynamic mechanics early warning model of rainfall induced bedding rock and soil landslide[J]. *Journal of Catastrophology*, 2015, 30(03): 38-42. (in Chinese)
- [4] LI H, XU Q, HE Y, et al. Prediction of landslide displacement with an ensemble-based extreme learning machine and copula models[J]. *Landslides*, 2018, 15(10): 2047-2059.
- [5] ZHOU Li, FAN Xuanmei, XU Qiang, et al. Numerical simulation and hazard prediction on movement process characteristics of Baige landslide in Jinsha River[J]. *Journal of Engineering Geology*, 2019, 27(6): 1395-1404. (in Chinese)
- [6] STRAUCH R, ISTANBULLUOGLU E, RIEDEL J. A new approach to mapping landslide hazards: a probabilistic integration of empirical and physically based models in the North Cascades of Washington, USA[J]. *Natural Hazards and Earth System Sciences*, 2019, 19(11): 2477-2495.
- [7] SANSARE D A, MHASKE S Y. Natural hazard assessment and mapping using remote sensing and QGIS tools for Mumbai city, India[J]. *Natural Hazards*, 2020, 100(3): 1117-1136.
- [8] DELANEY K B, EVANS S G. The 2000 Yigong landslide (Tibetan Plateau), rockslide-dammed lake and outburst flood: review, remote sensing analysis, and process modelling[J]. *Geomorphology*, 2015, 246: 377-393.
- [9] LIU Chun, FAN Xuanmei, ZHU Chenguang, et al. Discrete element modeling and simulation of 3-dimensional large-scale landslide—taking Xinmocun landslide as an example[J]. *Journal of Engineering Geology*, 2019, 27(6): 1362-

1370. (in Chinese)

- [10] WEI J, ZHAO Z, XU C, et al. Numerical investigation of landslide kinetics for the recent Mabian landslide (Sichuan, China)[J]. *Landslides*, 2019, 16(11): 2287-2298.
- [11] LU C, TANG C, CHAN Y, et al. Forecasting landslide hazard by the 3D discrete element method: A case study of the unstable slope in the Lushan hot spring district, central Taiwan[J]. *Engineering Geology*, 2014, 183: 14-30.
- [12] OUYANG C J, AN H, ZHOU S, et al. Insights from the failure and dynamic characteristics of two sequential landslides at Baige village along the Jinsha River, China[J]. *Landslides*, 2019.
- [13] ZHOU Qi, XU Qiang, ZHOU Shu, et al. Movement process of abrupt loess flowslide based on numerical simulation—a case study of Chenjia 8# on the Heifangtai Terrace[J]. *Mountain Research*, 2019, 37(04): 528-537. (in Chinese)
- [14] SONG Deguang, WU Ruian, MA Deqin, et al. Simulation analysis of landslide disaster movement process in Xigeda Formation, Luding County, Sichuan Province[J/OL]. *Geological Bulletin of China*, 2022: 1-13. (in Chinese)
- [15] ZOU Z, XIONG C, TANG H, et al. Prediction of landslide runout based on influencing factor analysis[J]. *Environmental Earth Sciences*, 2017, 76(21): 723.
- [16] XU Q, LI H, HE Y, et al. Comparison of data-driven models of loess landslide runout distance estimation[J]. *Bulletin of Engineering Geology and the Environment*, 2019, 78(2): 1281-1294.
- [17] GAO Yang, WEI Tongyao, LI Bin, et al. Dynamics process simulation of long run-out catastrophic landfill flowslide on December 20th, 2015 in Shenzhen, China[J]. *Hydrogeology & Engineering Geology*, 2019, 46(1): 129-138, 147. (in Chinese)
- [18] ZHOU Qi, XU Qiang, ZHOU Xiaopeng, et al. Research on the predicting hazard range of abrupt loess landslide—a case study of JJ6# landslide in Heifangtai Tableland[J]. *Journal of Catastrophology*, 2020, 35(01): 216-221. (in Chinese)
- [19] OUYANG C J, HE S M, XU Q, et al. A MacCormack-TVD finite difference method to simulate the mass flow in mountainous terrain with variable computational domain[J]. *Computers & Geosciences*, 2013, 52: 1-10.
- [20] OUYANG C J, HE S M, TANG C. Numerical analysis of dynamics of debris flow over erodible beds in Wenchuan earthquake-induced area[J]. *Engineering Geology*, 2015, 194: 62-72.